Synthesis and Properties of Vinyl Siloxane Modified Cresol Novolac Epoxy for Electronic Encapsulation

HORNG-JER TAI, J. B. WANG, JIUNN-HSIUNG CHEN, HUI-LUNG CHOU

Department of Chemical Engineering, I-Shou University, Number 1, Section 1, Hsueh-Cheng Road, Ta-Hsu Hsiang, KaoHsiung County, Taiwan 84008, Republic of China

Received 9 November 1999; accepted 19 March 2000

ABSTRACT: Vinyl siloxane (VS) modified cresol novolac epoxy (CNE) and cresol novolac hardener (CNH) resins are synthesized and both components are capable of further crosslinking. The reaction kinetics for both components are studied so that they can crosslink simultaneously in a designed synthesis procedure. Through careful adjustment of a triphenylphosphine dosage, the glass-transition temperature (T_g) of CNE/CNH resins can be effectively controlled. Phenomena characteristic of the existence of a diffusion-controlled reaction are also observed. The relationships between the T_g and crosslinking density for the CNE/CNH resin are explicitly revealed through gel content and swell ratio experiments. CNE/CNH resins with a higher T_g have lower equilibrium moisture uptake because of the higher fraction of free volume. The coefficient of diffusion also shows a similar but less apparent trend. The incorporation of VS incurs a 35% reduction in the equilibrium moisture uptake and a 20% reduction in the coefficient of diffusion for the modified resin. The VS-modified CNE/CNH resin possesses a lower Young's modulus and a higher strain at break than its unmodified counterpart does. This modified resin can help to alleviate the popcorning problems in integrated circuit packages, which results from hygrothermal stresses. © 2000 John Wiley & Sons, Inc. J Appl Polym Sci 79: 652–661, 2001

Key words: epoxy; vinyl siloxane; crosslinking density; moisture uptake; integrated circuit packaging

INTRODUCTION

Advantages in availability, cost, weight, and market lead time have given plastics more than 97% of the worldwide chip packaging market. *o*-Cresol-formaldehyde novolac epoxy (CNE) resins cured with cresol novolac hardeners (CNH), which have relatively low volumetric shrinkage upon polymerization, good thermal and dimensional stability, excellent moisture and chemical resistance, and superior electrical and mechanical properties, are often employed to encapsulate microelectronic devices.[1–3] The trend toward greater integration and functionality in the die is driving the need for packages of high pin counts and good heat dissipating capability. This places a great challenge on integrated circuit (IC) package materials. Among the common package reliability problems, moisture-induced delamination and cracking of the package during reflow soldering are two major issues. Ninety percent of failures occur at the material–material interface because of moisture, temperature cycling, and contamination.[1–3] A high level of stress is built up within the package as a result of the enhanced mismatch between the dissimilar materials in the package. At the same time, the evaporating moisture absorbed from the ambient by the epoxy-

Correspondence to: H.-J. Tai (hjtai@isu.edu.tw).

Journal of Applied Polymer Science, Vol. 79, 652–661 (2001)
© 2000 John Wiley & Sons, Inc.

based encapsulant causes a pressure buildup between the encapsulant and the chip pad. These effects, called the popcorning phenomenon, form paths for the ingress of contaminants and corrosive agents and compromise the long-term reliability of the package. In addition, hygrothermal aging-induced degradation also leads to a severe reduction in resin strength.[4]

Polysiloxanes are used extensively in IC packaging because of their good thermal stability, negligible thermal mismatch-induced internal package stress, resistance to UV degradation, and moisture repelling capability. They are employed as modifiers for epoxy resins in the hope that synergistic properties can be achieved. Various siloxanes, for example, aminosiloxane,[5] poly(dimethylsiloxane) (PDMS),[6–8] and PDMS-based thermoplastic polyurethane,[9] were incorporated into epoxy resins through grafting reactions. PDMS modifiers with carboxyl equivalent weights of less than 690 g/equiv mol were found to be completely miscible in the cured epoxy resin.[10] Polysiloxane-modified epoxy resins were reported to possess better thermal stability, a lower mechanical modulus, and the ability to absorb less moisture.[5–9] Other approaches for the synthesis of more reliable packaging materials include either use of low rigidity hardener in epoxy systems or synthesis of low thermal expansion coefficient polyimides.[11–13]

The stress buildup resulting from thermal mismatch can be qualitatively estimated using the following equation[14]:

$$\sigma = K \int (\alpha_r - \alpha_s) E_r \, dT \quad (1)$$

where σ is the interfacial stress between the encapsulant and the die, K is a constant, α_r is the linear coefficient of thermal expansion (LCTE) of the encapsulant, α_s is the LCTE of the silicon chip, and E_r is the flexural modulus of the encapsulant. The typical LCTE values for silicon chips and epoxy molding compounds are 2.6×10^{-6} and 17×10^{-6} K^{-1}, respectively.[15] At the same time, the evaporating moisture absorbed from the ambient by the epoxy-based encapsulant causes a pressure buildup between the encapsulant and the chip pad in the subsequent reflow soldering process. These popcorning phenomenon effects form paths for the ingress of contaminants and corrosive agents and compromise the long-term reliability of an IC package. To reduce thermal stresses in a package, it is necessary to reduce the values of α_r, E_r, or the moisture uptake of the encapsulant. The amount of moisture absorbed in a package is dependent on the magnitude of the resin diffusivity, as well as the equilibrium moisture uptake. The factors that affect the moisture transport process in epoxy resins include the polarity of the base resin, the catalyst used in the resin, and the resin nanovoid structure. Although resin polarity is the dominant factor in determining the equilibrium moisture uptake, there is a strong correlation between the absolute zero hole volume fraction and the equilibrium moisture uptake.[16] Some of the metal compounds used as catalysts in the epoxy system can also easily absorb moisture as their ligand.[17] In addition, the resin processing also affects the water content of a cured material to a great extent. In particular, the density and extent of crosslinking play a key role in the water uptake during thermal spikes. Besides the equilibrium moisture uptake, the diffusivity of moisture in the resin is another important factor that affects package reliability that is often overlooked. The period between postcure treatment and reflow soldering of encapsulated packages is usually a couple of days. Encapsulants with a lower diffusivity will absorb less moisture. The diffusion process in an epoxy resin is complicated by the existence of a microstructure difference in the resin. Different modes of moisture diffusion exist in the phases of different crosslinking densities.[18] How resin polarity and chain topology affect the diffusivity remains an important issue.

In this study a vinyl siloxane (VS) grafted CNE prepolymer was synthesized, and the VS and epoxy components were both capable of further crosslinking. A silane compatiblizer for enhancing the interphase reaction was added. The reaction kinetics for the crosslinking reactions in both components were studied, which enabled us to prepare the modified resin in a procedure where both components reacted simultaneously. The effects of the glass-transition temperature (T_g) and the addition of VS on the mechanical and moisture transport properties of the resins were also discussed.

EXPERIMENTAL

Materials

The epoxy resin used was CNE supplied by ChangChun Plastics (CNE-200EL, grade F, epoxy

equivalent = 200 g/equiv, number average functionality = 8). The CNH was also supplied by ChangChun Plastics (HOCN-200, hydroxyl equivalent = 110 g/equiv, number average functionality = 9). The VS used was X-21-5999 supplied by Shin-Etsu Co. (vinyl equivalent = 1.3×10^{-4} mol/g, viscosity at 25°C = 757 cs). Triphenylphosphine (TPP, Ph_3P) and methacrylic acid (MAA) were purchased from Aldrich. The TPP was used as a curing accelerator for the CNE/CNH system. Benzoyl peroxide; 1,1 di-(*tert*-butylperoxy) 3,3,5-trimethyl cyclohexane (Lupersol 231); *n*-butyl-4,4-di-(*tert*-butylperoxy) valerate (Lupersol 230); dicumyl peroxide; 2,5 dimethyl-2,5-di-(*tert*-butylperoxy) hexane (Lupersol 101); and 2,5 dimethyl-2,5-di-(*tert*-butylperoxy) hexyne-3 (Lupersol 130) were purchased from Atochem Inc. The A-1 catalyst used was (ethyl)triphenyl phosphonium acetate acetic acid complex, which was also supplied by ChangChun Plastics. 3-Glycidoxypropyl trimethoxysilane was supplied by Chisso Corp. The silane served as a compatiblizer for the epoxy resins and the polysiloxane modifier.

Methods

Preparation of Unmodified Epoxy Resins

A 500-mL four-necked round-bottom flask equipped with a heating mantle, mechanical stirrer, thermocouple, and temperature controller was used as a reactor. To avoid oxidation and hydrolysis, the reactor was purged with high purity nitrogen gas and maintained at 120°C throughout the process. Stoichiometric amounts of CNE and CNH, along with 0.1–1 wt % TPP, were added to the reactor mentioned above. The mixing was maintained for 0.5 h.

Grafting of MAA onto Epoxy Resins

The same reactor and conditions were applied for the preparation of the MAA-grafted epoxy. One hundred twenty-eight grams of CNE was added, followed by the dropwise addition of 1.833 g of MAA and 0.267 g of A-1 catalyst over a period of 0.5 h. The reaction was maintained for an additional 1.5 h. Completion of the reaction was confirmed by no trace of MAA being detected by gas chromatography and the intensity of the absorption bands of oxirane at 882 and 917 cm^{-1} was reduced because of the ring-opening reaction of the epoxides with the carboxyl groups. MAA was grafted onto the epoxy resin in order to later react with the VS.

Preparation of VS-Modified Epoxy Resins

Stoichiometric amounts of MAA-grafted CNE and CNH, along with 0.1 wt % TPP, were added to the reactor mentioned above. Then 13 wt % VS, 0.15 wt % 3-glycidoxypropyl trimethoxysilane, and 0.3 wt % 2,5 dimethyl-2,5-di-(*tert*-butylperoxy) hexane were added. The mixing was maintained at 120°C for 0.5 h.

Curing Procedure of Epoxy Resins

The powders of unmodified and VS-modified CNE/CNH resins were cured in a mold under a 50 kg/cm^2 pressure. The temperature was first set to 80°C and maintained for 8 h. The temperature was then raised to 120°C for 0.5 h and then to 170°C for an additional 0.5 h. The temperature was then set to 220°C and was maintained for 4 h for a postcure. To relax the thermal molding stress, the specimens were taken out of the mold and placed into a vacuum oven for 0.5 h at 190°C.

Measurement and Testing

The variation in the T_g as a function of TPP accelerator dosage was studied using DSC according to ASTM D3418-82. The midpoint ($\frac{1}{2}\Delta C_p$) at the step increment in the DSC curve was taken as the T_g. A dynamic DSC scan method was used to follow the reaction kinetics and heat of reaction. Unreacted specimens were scanned from 25 to 220°C at heating rates of 10 and 20°C/min. The gel content and swell ratio of the specimens with various T_g values were measured using the reflux extraction method. A sample of about 0.3 g was placed in a pouch made of 120 mesh stainless steel cloth and immersed in boiling tetrahydrofuran (THF) for 24 h. The amount of remaining gel and the value of the swell ratio were then calculated in a way similar to that described in ASTM D2765-90. The LCTE was measured using a Perkin–Elmer DMA 7e in the TMA mode. The 4 mm thick specimens were placed under a quartz probe using a contact force of 2 mN, and the vertical dimension (thickness) was measured as the temperature was increased at a rate of 5°C/min. The mechanical properties were measured using an Instron 4411 universal testing machine in accordance with ASTM D638M-93. Type M-1 specimens were tested and their Young's moduli, strains at break, and ultimate tensile strengths were obtained at a crosshead speed of 5 mm/min. In the moisture absorption experiments the $40 \times 20 \times 4$ mm^3 specimens were placed in an 85°C

and 85% relative humidity chamber.[19] The weight gain was monitored as a function of time. Prior to the absorption experiments, samples were dried in a vacuum oven for 7 days at 50°C to remove excess moisture.

RESULTS AND DISCUSSION

Matching of Crosslinking Rates of CNE/CNH and VS

In formulating the VS-modified CNE/CNH resins, time–temperature profiles for both the prepolymer preparation and the final curing process must be well planned. The resin must be stable enough at the preparation temperature of 120°C. Meanwhile, most molding processes demand the cure time for the resin (postcure time not included) to be no more than 5 min at 175°C. In addition, because two reactions (crosslinking of VS and crosslinking of CNE/CNH resins) are involved in curing the VS-modified CNE/CNH resin, the kinetics for both reactions must be quantified. Figure 1 shows some typical reaction curves for the CNE/CNH resin with various amounts of TPP and for the VS with various peroxide initiators at a dosage of 1 wt %. A simple nth order was used to fit each reaction curve:

$$\frac{dX}{dt} = A \exp\left(\frac{E}{RT}\right) \quad (2)$$

where X is the degree of conversion, A is the frequency factor, and E is the activation energy. The values of the fitted kinetic parameters for both reacting systems are shown in Tables I and II, respectively. These values were not intended to be used for the reaction mechanism study but instead were used as a quantitative tool for process synthesis. The formulation and processing procedures for the VS-modified CNE/CNH resin described in the Experimental section were determined by implementing the kinetic calculation. The two reactions should take place simultaneously, in the hope that an interpenetrating polymer network like structure could be obtained to prevent large-scale phase separation.

In the DSC experiments, it was found that the TPP concentration affected not only the crosslinking reaction rate, but also the T_g of the CNE/CNH resins. Figure 2 shows the heat of reaction, the DSC exotherm peak temperature, and the resultant T_g of CNE/CNH resins at different concentrations of TPP. It can be seen that the DSC exotherm peak temperature decreases with increasing TPP concentration: when a higher amount of TPP was added, the crosslinking reaction took place at a lower temperature and at a higher rate; therefore, a higher extent of reaction was achieved and a higher amount of reaction heat was released. Consequently, the peak temperature followed a trend opposite to the heat of reaction in Figure 2. Also, the T_g increases monotonically with increasing TPP concentration. Because it is generally considered to be true for most thermosetting polymers that there is a one to one relationship between the T_g and the degree of conversion, regardless of the cure path,[20–22] a higher T_g implies that a higher degree of conversion has been achieved. But the heat of reaction curve does not show such a trend. Instead, the heat of reaction initially increases with increasing TPP concentration and then levels off as the TPP concentration exceeds 0.3 wt %. This indicates that a diffusion-controlled reaction mechanism also played an important roll. Because the diffusion-controlled reaction rate was slow, the reaction heat was too low to be detected by the DSC. TPP not only accelerated the chemical ki-

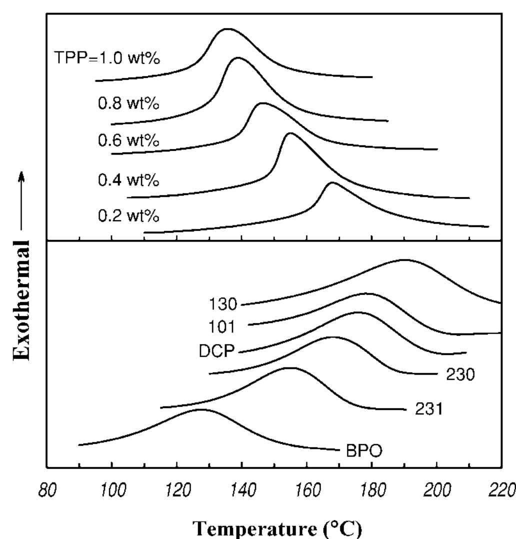

Figure 1 Typical DSC exotherms for CNE/CNH resins with various amounts of TPP and for VS with various peroxide initiators at a dosage of 1 wt %. The designations are (130) 2,5 dimethyl-2,5-di-(*tert*-butylperoxy) hexyne-3; (101) 2,5 dimethyl-2,5-di-(*tert*-butylperoxy) hexane; (DCP) dicumyl peroxide; (230) *n*-butyl-4,4-di-(*tert*-butylperoxy) valerate; (231) 1,1 di-(*tert*-butylperoxy) 3,3,5-trimethyl cyclohexane; and (BPO) benzoyl peroxide.

Table I Kinetic Parameters for Crosslinking Reaction of Vinyl Siloxane

Peroxide	A (s^{-1})	E/R (K^{-1})	n
Benzoyl peroxide	1.166×10^{14}	14,687	1.173
1,1 Di-(*tert*-butyl peroxy)3,3,5-trimethyl-cyclohexane	3.776×10^{16}	18,122	1.157
n-Butyl-4,4-di-(*tert*-butylperoxy) valerate	1.927×10^{16}	19,413	1.082
Dicumyl peroxide	7.398×10^{15}	18,344	0.984
2,5 Dimethyl-2,5-di-(*tert*-butylperoxy) hexane	6.465×10^{13}	16,444	1.157
2,5 Dimethyl-2,5-di-(*tert*-butylperoxy) hexyne-3	1.731×10^{12}	15,251	1.022

netic controlled reaction, but it also accelerated the diffusion-controlled reaction; thus, a higher degree of conversion was achieved with increasing TPP concentration. We could then control the T_g of the CNE/CNH resin by adjusting the amount of TPP in the resin. The resin could be placed in a high temperature environment for a certain period of time without an appreciable change of the T_g.

Gel Content and Swell Ratio

As a polymerization reaction proceeds, low molecular weight monomers are consumed and the system average molecular weight increases. When the degree of conversion reaches the gel point, the continuing structure buildup leads to an infinite network (gel). The gel fraction increases at the expense of the sol fraction as the polymerization reaction continues. An experimental approach to understand this gel–sol partition phenomenon is to measure the gel content or swell ratio by dissolving the network in a good shows that gelation occurred at the very early stage of polymerization, which is not surprising because the resin has a very high functionality and a high initial molecular weight. The gel content increases dramatically as the reaction proceeds past the gel point; then it levels off in a short period because its value is close to 100%. If the distribution of chain lengths between crosslinks is Gaussian, the crosslinking density can be estimated quantitatively from a gel content value by using the Inokuti equation[23]:

$$w_{\text{gel}} = 1 - \left(\frac{\sigma}{\sigma + \rho u w_{\text{gel}}}\right)^{\sigma+1} \tag{3}$$

where w_{gel} is the gel content; and σ is a measure of the distribution breadth, which is defined as

$$\sigma = \frac{1}{(M_w/M_n) - 1} = \frac{M_n}{M_w - M_n} \tag{4}$$

where M_w is the weight-average molecular weight; M_n is the number-average molecular weight; ρ is the crosslinking density, defined as the fraction of units that bear tribranching points[24]; and u is the initial number-average chain length. For a rigid and highly crosslinked system like the CNE/CNH resin, the Inokuti equation can only be qualitative. If the initial molecular weight distribution is so sharp that it

Table II Kinetic Parameters for Crosslinking Reaction of CNE/CNH Resins

Amount of TPP (wt %)	A (s^{-1})	E/R (K^{-1})	n
0.1	8.926×10^{12}	15,944	1.363
0.2	7.145×10^{13}	16,137	1.450
0.3	1.961×10^{18}	20,356	1.720
0.4	7.417×10^{14}	16,674	1.510

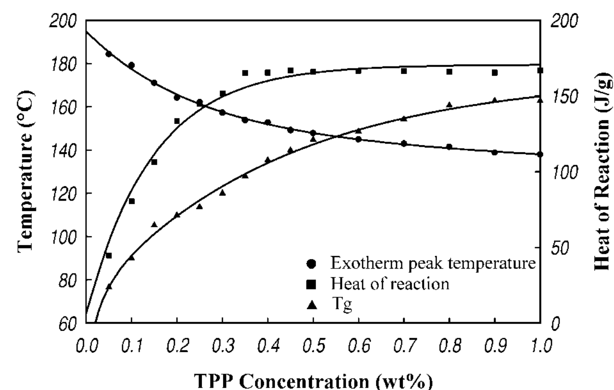

Figure 2 The heat of reaction, DSC exotherm peak temperature, and T_g for the CNE/CNH resin as functions of the TPP concentration.

approaches infinity, then the Inokuti equation can be reduced to

$$\rho u = -\frac{\ln(1 - w_{\text{gel}})}{w_{\text{gel}}} \tag{5}$$

Because u is a constant, ρ is proportional to the right-hand side of the above equation. We found that the gel content experiment performed better when evaluating the crosslinking density of the CNE/CNH system in the early stage of a crosslinking reaction. As the value of the gel content reached 90%, the involved experimental error prevented us from accurately estimating the crosslinking density, even qualitatively.

On the contrary, the swell ratio experiment performed more adequately when assessing the crosslinking density in the high conversion regime. We can see from Figure 3 that although the gel content leveled off when the T_g value was higher than 80°C, the swell ratio continued to decrease. The crosslinking density was estimated using the Flory–Rehner equation[25,26]:

$$v_s = -\frac{\ln(1 - v_r) + v_r + \chi v_r^2}{V_1[v_r^{1/3} - (2/f)v_r]} \tag{6}$$

where v_s is the effective network chains per unit volume of gel, v_r is the volume fraction of polymers in the swollen network (the inverse of the swell ratio), V_1 is the molar volume of THF (89.28 mL/mol at 65°C), χ is the coefficient of interaction between THF and CNE/CNH, and f is the crosslinking functionality. The χ was estimated using[27]

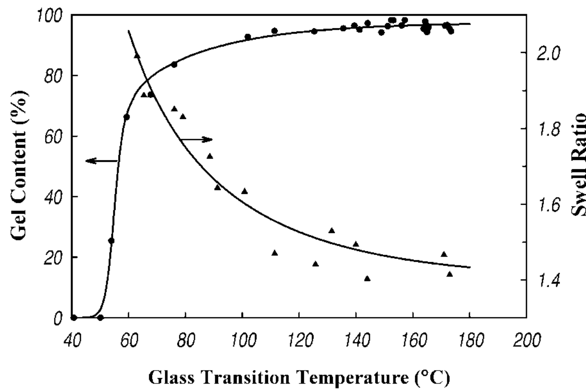

Figure 3 The gel content and swell ratio as functions of the T_g for the CNE/CNH resin.

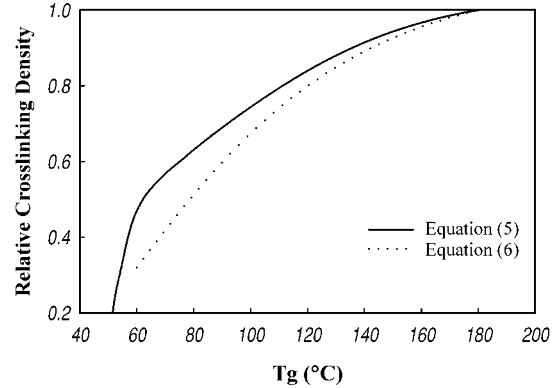

Figure 4 The relative crosslinking density as a function of the T_g as calculated using eqs. (5) and (6).

$$\chi \approx 0.34 + \frac{V_1}{RT}(\delta_P - \delta_S)^2 \tag{7}$$

The solubility parameter δ_S of THF is 19.6 $J^{1/2}/mL^{1/2}$. The solubility parameter δ_P of the crosslinked CNE/CNH resin was difficult to measure and was assumed to be equal to δ_S. Again, the Flory–Rehner equation can serve only for a qualitative purpose because of the high rigidity and high crosslinking density of this CNE/CNH system. The estimated relative crosslinking densities for resins of various T_g values using eqs. (5) and (6) are shown in Figure 4. The values in Figure 4 were normalized by taking the highest crosslinking density value as 1 for each individual curve. This figure clearly shows that the resin crosslinking density increases monotonically with the T_g. Together with Figure 3, we see that, when gelation occurs, there is a dramatic increase in crosslinking density but only a minor increase in the T_g.

Moisture Uptake

CNE/CNH resins of different T_g values were prepared and subjected to an 85% relative humidity and 85°C environment. Figure 5 shows the typical moisture uptake curves. The moisture content increases rapidly during the initial stages of diffusion and levels off to a saturation level. It is important to note that the higher the T_g, the lower the equilibrium moisture uptake. Assuming the diffusion behavior followed a Fickian pattern, the moisture concentration in a slab can be shown to be[28]

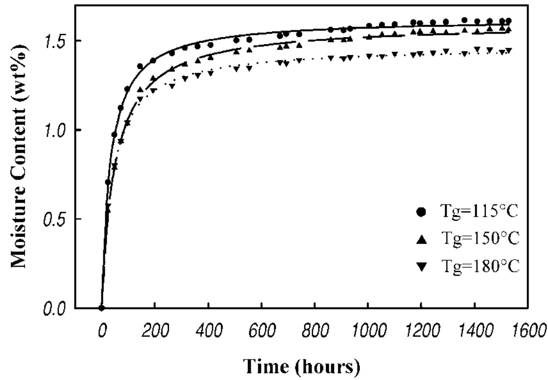

Figure 5 Typical moisture–time profiles in the moisture uptake experiments for the CNE/CNH resin with various T_g values.

$$\frac{\bar{c}(t)}{c_o} = 1 - \frac{8}{\pi^2} \sum_{j=0}^{\infty} \frac{1}{(2j+1)^2} \exp\left[-\left(\frac{(2j+1)\pi}{h}\right)^2 Dt\right] \quad (8)$$

where $c(t)$ is the average concentration at a time t, c_o is the saturation concentration at the surface, h is the slab thickness, and D is the diffusion coefficient. The calculated D values and the equilibrium moisture uptake are shown in Figure 6. The CNE/CNH resin absorbed only a low level of moisture of 1–1.5 wt %. In contrast, the epoxy/amine systems can absorb 2–7 wt % moisture.[16–18,29] This is one of the reasons why CNE/CNH systems are chosen as IC packaging materials. But even this level of moisture content causes many reliability problems for IC packages. It is obvious from Figure 6 that the equilibrium moisture uptake decreases with increasing T_g. The value of the diffusion coefficient also decreases somewhat with increasing T_g, but the trend is less certain. The D values calculated here using eq. (8) were in good agreement with those reported by Shook (2.2–3.4×10^{-8} cm^2/s) using a different approach for packages encapsulated with similar commercial epoxy systems.[30] Because of the low moisture content, there is no need to treat the diffusion coefficient as concentration dependent and to incorporate a plasticization factor into it.[31] Morel et al. showed that the most important factor in determining the equilibrium moisture uptake is the resin polarity,[32] but the volume fraction of nanovoids inside the resin also influences the equilibrium moisture uptake.[16] Resins of lower T_g, hence of lower overall crosslinking density, possess a higher volume fraction of nanovoids to accommodate more unbound moisture. This is the reason why resins of lower T_g absorb higher amounts of moisture. Because the moisture uptake experiments were performed at a temperature lower than the T_g of the resins, this could be the reason why the diffusion coefficients did not show an obvious decreasing trend with increasing T_g. Although Soles et al. used various curing agents to synthesize epoxy resins of constant polarity in order to study the influence of nanovoids on the equilibrium moisture uptake,[16] we demonstrate here that resins of constant polarity but different topology can also be synthesized by adjusting the amount of curing accelerator in the CNE/CNH system.

VS-Modified CNE/CNH Resins

In order to synthesize a resin with a lower modulus and less hygroscopicity, a flexible VS modifier was added to modify the CNE/CNH resin. Various measures for incorporating the VS modifier into the CNE/CNH matrix were tried. Table III shows the mechanical properties of resins synthesized using different approaches. Because the VS modifier is completely immiscible with the CNE/CNH resin, good mechanical properties could not be achieved by direct mixing of the two materials (the resin designated as blend in Table III). When MAA was grafted onto CNE (the graft resin in Table III), the CNE and VS components both possessed the C═C functionality. Interphase chemical bonds were formed and made the boundary between the CNE/CNH and VS phases less distinctive. The addition of 3-glycidoxypropyl trimethoxysilane, which served as a coupling

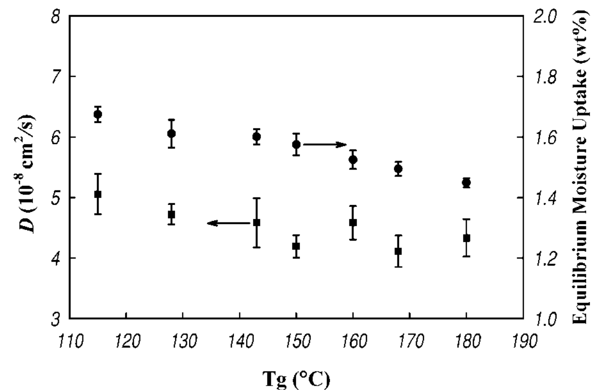

Figure 6 The coefficient of diffusion D and equilibrium moisture uptake as functions of the T_g for the CNE/CNH resin.

Table III Mechanical Properties for Resins Synthesized Using Different Methods

	Control[a]	Blend[b]	Graft[c]	Blend/C[d]	Graft/C[e]
Young's modulus (GPa)	0.95	0.76	0.82	0.81	0.8
Tensile strength (MPa)	28	13	20	17	26
Strain at break (%)	3.11	1.95	2.7	1.74	3.28
T_g (°C)	182	183	184	181	183

[a] Stoichiometric amounts of CNE and CNH, along with 0.1 wt % TPP.
[b] Same as the control [a] with the addition of 13 wt % VS and 0.3 wt % 2,5 dimethyl-2,5-di-(*tert*-butylperoxy) hexane.
[c] Same as the blend [b] but CNE is replaced by MAA-grafted CNE.
[d] Same as the blend [b] with the addition of 0.15 wt % 3-glycidoxypropyl trimethoxysilane.
[e] Same as the graft [c] with the addition of 0.15 wt % 3-glycidoxypropyl trimethoxysilane.

agent for the two phases, promoted the mechanical properties substantially. It worked equally well for both the direct-mixed (blend/C) and MAA graft modified (graft/C) resins. The increase in toughness for the rubber-modified epoxy resin can be ascribed to the two energy-dissipating mechanisms: the cavitation at the particle–matrix interface and the multiple plastic shear yielding in the matrix initiated by the stress concentration associated with the rubbery particles.[33] The improvement in the adhesion between the matrix–rubber interfaces promotes the extent of cavitation, which was proved to be very effective in promoting the toughness of the rubber-toughened epoxy resin.[34] For the graft/C resin in Table III, the silane enhanced the interphase reaction and more interphase chemical bonds were formed. The resin synthesized this way possessed a lower Young's modulus but a higher strain at break, yet the reduction in tensile strength was minimal. The T_g values for each resin were essentially identical, indicating the existence of a two-phase structure. Because the graft/C resin possessed the most balanced mechanical properties among all the modified resins, it was used for comparison with the control resin for a series of other tests.

During reflow soldering, the entire package was heated to temperatures as high as 230°C. It is important that the package still maintain its integrity. The high-temperature mechanical properties of the modified resin should be comparable to those of the unmodified one. Figure 7 shows the results of mechanical properties tested at 25, 50, 75, 100, and 140°C for the control and graft/C resins. We can see that the property–temperature profiles for the two resins are almost parallel to each other. No change in the T_g and the parallel mechanical properties over temperatures implies that the service temperature for the VS-modified resin was not sacrificed.

Figure 8 shows the typical moisture uptake curves for the control and graft/C resins with the same T_g (180°C). It is quite obvious that the incorporation of the VS modifier into the CNE/CNH matrix profoundly reduced the amount of moisture uptake. The equilibrium moisture uptake was reduced from 1.45 to 0.93 wt %. Notice that the level of moisture uptake in the graft/C resin based on the CNE/CNH content (1.07 wt %) is still significantly lower than that in the control resin (1.45 wt %). Assuming that the VS component does not absorb moisture at all, the incorporation of the VS modifier also made the CNE/CNH phase absorb much less moisture. The diffusion coefficients for the control and graft/C resins were 4.33 $\times 10^{-8}$ and 3.44 $\times 10^{-8}$ cm^2/s, respectively, as calculated by using eq. (8). The addition of nonpolar VS not only made the graft/C resin become

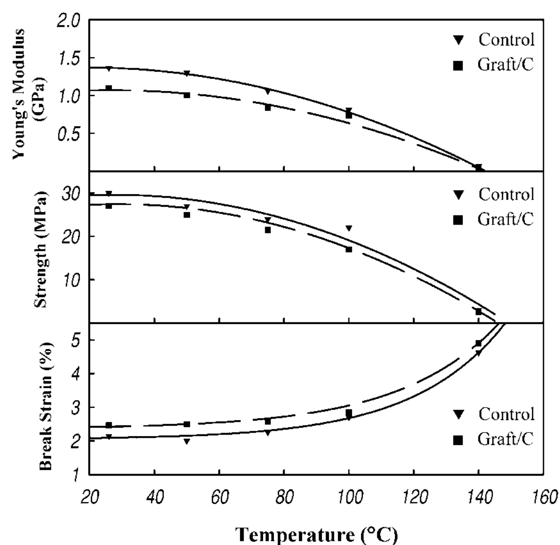

Figure 7 The Young's modulus, ultimate tensile strength, and strain at break as functions of temperature for the control and graft/C resins.

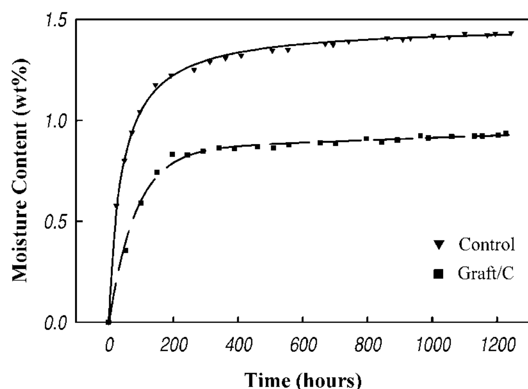

Figure 8 Typical moisture–time profiles in the moisture uptake experiments for the control and graft/C resins.

less hygroscopic, but it also incurred a reduction in the diffusion coefficient. The detour around the nonhygroscopic VS phase made the diffusion path longer and reduced the overall diffusion coefficient.

The linear coefficients of thermal expansion as functions of the T_g for the two resins were compared. For glassy polymers, two distinct LCTEs were found over temperature ranges below and above their T_g, which are usually denoted as α_1 and α_2, respectively. As shown in Figure 9, the incorporation of flexible VS raised the values of the α_1 and α_2 for the resins. The internal thermal stress-induced increase of the local free volume and the building of high LCTE siloxane molecules into the network structure were the two effects that caused the increase in LCTE for the modified resin.[10] The epoxy molding compounds applied in the IC packaging process usually incorporate a large amount of silica fillers. The effect of the incorporation of VS on the LCTE reverses when silica fillers are added.[10] The higher internal thermal stress near the polymer–filler interface causes the siloxane-modified epoxy molding compound to have a lower LCTE than its unmodified counterpart. The effect of the T_g on the LCTE of both the modified and the unmodified resins was similar, judging from the similar slopes observed in the LCTE–T_g curves for both resins. Resins of higher T_g have higher fractions of free volume and thus have higher LCTE values.

CONCLUSIONS

In this study, we synthesized a VS-modified CNE/CNH resins with both components capable of further crosslinking. The reaction kinetics for VS and CNE/CNH systems was studied in order to plan an effective synthesis procedure. The reaction rates could be controlled by adjusting the TPP concentration for the CNE/CNH system and by using a variety of peroxide initiators for the VS system. Through adjusting the TPP dosage, the CNE/CNH resin with controlled T_g values could be obtained. The gel content and swell ratio experiments were adequate for revelation of the crosslink structure for the CNE/CNH system. The crosslinking density increased dramatically when gelation occurred while the T_g was mildly increased. The equilibrium moisture uptake and coefficient of diffusion for the CNE/CNH resin also showed a decreasing trend with the T_g. The use of the coupling agent 3-glycidoxypropyl trimethoxysilane was very effective in enhancing the interphase reaction between the VS and MAA-grafted CNE. The VS-modified resin possesses balanced mechanical properties: a lower Young's modulus so that the interfacial thermal stress was reduced; a higher strain at break implied a better resin toughness; and the tensile strength suffered only a minor decrease. The T_g values were close to each other for both the modified and unmodified resins, and their mechanical property–temperature profiles were almost parallel to each other. Most important of all, the equilibrium moisture uptake and coefficient of diffusion for the VS-modified CNE/CNH resin were both reduced to a great extent. Overall, we successfully modified the CNE/CNH resin by properly incorporating a VS into the network. The

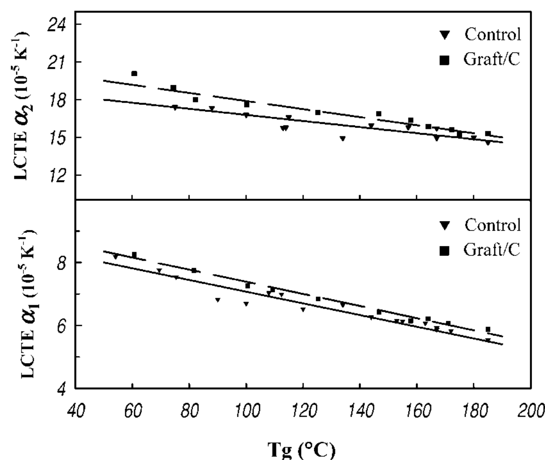

Figure 9 The linear coefficients of thermal expansion (W_1 and W_2) as functions of the T_g for the control and graft/C resins.

newly synthesized resin has improved hygrothermal and thermal mechanical properties without any sacrifice in its service temperatures.

REFERENCES

1. Enlow, L. R.; Swanson, D. W.; Naito, C. M. Microelectron Reliabil 1999, 39, 515.
2. Tay, A. A. O.; Tan, G. L.; Lim, T. B. IEEE Trans Compos Pack Manufact Technol Part B 1994, 17, 201.
3. Gannamani, R.; Pecht, M. IEEE Trans Compos Pack Manufact Technol Part A 1996, 19, 194.
4. Xiao, G. Z.; Shanahan, M. E. R. J Polym Sci Polym Phys Ed 1997, 35, 2659.
5. Shieh, J. Y.; Ho, T. H.; Wang, C. S. Angew Makromol Chem 1995, 224, 21.
6. Sung, P. H.; Lin, C. Y. Eur Polym J 1997, 33, 231.
7. Lin, L. L.; Ho, T. H.; Wang, C. S. Polymer 1997, 38, 1997.
8. Lin, S. T.; Huang, S. K. Eur Polym J 1997, 33, 365.
9. Ho, T. H.; Wang, C. S. Polymer 1996, 37, 2733.
10. Meijerink, J. I.; Eguchi, S.; Ogata, M.; Ishii, T.; Amagi, T.; Numata, S.; Sashima, H. Polymer 1994, 35, 179.
11. Numata, S.; Kinjo, N. Polym Eng Sci 1988, 28, 906.
12. Matsumoto, A.; Hasegawa, K.; Fukuta, A. Polym Int 1993, 31, 275.
13. Ogata, M.; Kinjo, N.; Kawata, T. J Appl Polym Sci 1993, 48, 583.
14. Kuwata, K.; Ito, K.; Tabata, H. IEEE Trans Compos Hybrids Manfact Technol 1985, 8, 486.
15. Manzione, L. T. Plastic Packaging of Microelectronic Devices; Van Nostrand Reinhold: New York, 1990; p 63.
16. Soles, C. L.; Chang, F. T.; Bolan, B. A.; Hristov, H. A.; Gidley, D. W.; Yee, A. F. J Polym Sci 1998, 36, 3035.
17. Wong, T. C.; Broatman, L. J. Polym Eng Sci 1985, 25, 521.
18. Vanlandingham, M. R.; Eduljee, R. F.; Gillespie, J. W., Jr. J Appl Polym Sci 1999, 71, 187.
19. JEDEC Standard Test Method 112, Moisture-Induced Stress Sensitivity for Plastic Surface Mount Devices; Apr. 1994, JEDEC Solid State Technology Association, Arlington, VA.
20. Hale, A.; Macosko, C. W.; Bair, H. E. Macromolecules 1991 24, 2610.
21. Wang, X.; Gillham, J. K. J Appl Polym Sci 1992, 45, 2127.
22. Lunak, S.; Vladyka, J.; Dusek, K. Polymer 1978, 19, 931.
23. Inokuti, M. J Chem Phys 1963, 12, 2999.
24. Tobita, H. J Polym Sci Polym Phys Ed 1995, 33, 1191.
25. Flory, P. J.; Rehner, J. J Chem Phys 1943, 11, 521.
26. Flory, P. J. J Chem Phys 1950, 18, 108.
27. Van Krevelen, D. W. Properties of Polymers; Elsevier Science B. V.: Amsterdam, 1990; 3rd ed., p 189.
28. Shewmon, P. S. Diffusion in Solids; McGraw–Hill: New York, 1963; p 18.
29. Diamant, Y.; Marom, G.; Broat, L. J. J Appl Polym Sci 1981, 26, 3015.
30. Shook, R. L. In Proceedings of the 30th Reliability Physics Symposium; 1992; p 157, IEEE Inc., Piscataway, NJ.
31. Marais, S.; Metayer, M.; Labbe, M. Polym Eng Sci 1999, 39, 1508.
32. Morel, E.; Bellinger, V.; Verdu, J. Polymer 1985, 26, 1719.
33. Pearson, R. A.; Yee, A. F. J Mater Sci 1989, 24, 2571.
34. Chen, T. K.; Jan, Y. H. Polym Eng Sci 1991, 31, 577.